Aerospace Systems
https://doi.org/10.1007/s42401-021-00101-1

ORIGINAL PAPER

Design of an unmanned aircraft system for high-altitude 1 kW fuel cell power system

William A. Reid[1] · **Ibrahim M. Albayati**[1]

Received: 21 December 2020 / Revised: 29 June 2021 / Accepted: 10 August 2021

Abstract

A proton exchange membrane (PEM) fuel cell is particularly considered as a prime power supply for a fuel cell-powered unmanned aircraft system (UAS) as it possesses a very high-power density in comparison with other fuel cell types, hence a high potential to be used for high altitude long endurance (HALE) UAS flights. This paper will focus on examining the design requirements for the UAS-based 1 kW PEM fuel cell for high altitude operation (10–11 km), which can be correlated into a quantitative data to produce a design constraints diagram. The maximum take-off mass, endurance, and geometries for potential UAS design are estimated. Four different geometrical design profiles are developed and presented. The resulting geometries are analysed and the design parameters of the estimated 1 kW design yielded an aircraft of maximum take-off mass 34.8 kg, wingspan of 10.4 m, cruising speed 20 m/s, stall speed 11.23 m/s, and maximum endurance of 4 h. The constraint diagram deploys these assumptions as well as values generated through the design calculations to form a possible design of which the 1 kW UAS falls slightly outside of the possible design space; this is due to the minimum thrust-to-weight ratio required to achieve the desired service ceiling; however, further alterations and adjustments on the design and mission requirements are provided to place the design of the UAS within the possible design space.

Keywords Constraints design · Fuselage and wingspan · High altitude · PEM fuel cell · Mass estimation · UAS

Abbreviations

A	Area of the propeller's rotation path (m^2)
AR	Aspect ratio (-)
b	Wingspan (m)
b_f	Maximum width of fuselage (m)
C_{Dmin}	Minimum drag coefficient (-)
C_{Lmax}	Maximum lift coefficient (-)
C_{root}	Chord root (m)
C_{tip}	Chord tip (m)
D_{ave}	Average diameter of fuselage (m)
d_{to}	Take-off distance (m)
e	Oswald efficiency number (-)
FR	Finesse ratio (-)
G	Gravity force (N)
GTOM	Gross take-off mass (kg)
h_f	Maximum depth of fuselage (m)
HP	Horsepower (hp)
k	Lift induced drag constant (-)
K_λ	Correction factor of shell mass (-)
l_f	Length of fuselage (m)
l_t	Distance between ¼ chord points of wing root and horizontal (m)
M	Maximum take-off mass (kg)
MAC	Mean aerodynamic chord (m)
P_d	Propeller diameter (m)
P_O	Power output (W)
P_S	Power supply (W)
q	Dynamic pressure (kg/m^2)
S or SWING	Wing surface area (m^2)
S_G	Gross shell area (m^2)
T_{root}	Theoretical root thickness (m)
T_{sm}	Maximum static thrust (N)
T/W	Thrust-to-weight ratio (-)
V	Airspeed (cruising speed) (m/s)
V_D	Design dive speed (m/s)
V_{So}	Stall speed (m/s)
V_V	Vertical speed (m/s)
W	Weight (N)
W_G	Gross shell mass (kg)

✉ Ibrahim M. Albayati
ialbayati@lincoln.ac.uk

William A. Reid
15624011@students.lincoln.ac.uk

[1] School of Engineering, University of Lincoln, Brayford Pool, Lincoln LN6 7TS, UK

Published online: 22 October 2021

W_{fr}	Gross frame mass: (kg)
W_{sk}	Gross skin mass: (kg)
W_{str}	Gross stringer and longeron mass (kg)
(W/S) or W_s	Wing loading (N/m^2)
W_{wing}	Wing mass (kg)
XLF or N_{ult}	Ultimate load factor (-)
ρ	Density of air (kg/m^3)
ρ_{SL}	Density of air at sea level (kg/m^3)
η_m	Efficiency of motor (-)
η_p	Efficiency of propeller (-)
η_{PEM}	Efficiency of proton exchange membrane fuel cell (-)
λ	Taper ratio (-)

1 Introduction

An unmanned aircraft system (UAS) is an integration of the unmanned aerial vehicle (UAV) and a control system which allows users to remote control the aircraft. The UAS will enable the operator to obtain a real-time photo/video footage for large areas and from different altitudes. Some missions that are carried out by the UAS require the capability of the system to operate at high altitudes reaching up to 11 km, and for several days endurance, this type of mission is often referred to high altitude and long endurance (HALE) mission [1].

The first development of the UAS began during the World War I; however, none of these aircraft have progressed into the testing phase until before the end of the war. During the 1930s, the experiments on the radio-controlled unmanned aircraft systems were carried out and the Royal Navy used an adapted DH82 Tiger Moth named Queen Bees [1]. Post-World War II, production of basic training target (BTT) UAS was manufactured, with the first BTT being converted to an aerial reconnaissance drone by the mid of the 1950s, and the aircraft is now designated as MQM-57 Falconer. Furthermore, in the 1982, the US Air Force and Israeli Air Force began a joint project whereby they created a UAS by the name of RQ2 Pioneer. The U.S. Department of Defence spent $3 billion during the 1990s on UAS research and operations. In 2001, a UAS named MQ-1 Predator which can carry attack missiles was manufactured; since then, an updated version of the MQ-1 Predator has been innovated and named as MQ-9 Reaper with a greater focus on the utilisation of weaponry in service [2].

The methodology of a conventional aircraft design remains similar across the entire aviation community with perhaps slight differences in the order of operations and design requirements [3, 4]. Tsach et al [5] developed a design of a transonic HALE UAV for intelligence missions focusing on surveillance military and civilian missions with relatively large payloads of up to 250 kg and for a short flight mission of 50 h. Altman [6] developed a robust design methodology and performance evaluation for low-speed HALE UAVs for the environmental and military reconnaissance or communication applications. Dababneh et al. [7] reviewed several different techniques for wing mass estimations, one of which using statistical data from other aircrafts which yields a usable equation for wing mass estimations. The assumed material used in the mathematical model is aluminium and the aircrafts are assumed to be high-speed aircrafts.

Fuel cell is a promising choice for the replacement of the conventional combustion engines as they offer a higher overall performance efficiency. Proton exchange membrane (PEM) fuel cells use hydrogen and oxygen to produce DC power, thus can be used in aircraft as they possess high-power density between 0.5 and 2.5 Wcm^{-2} in comparison with other fuel cells. This means that PEM fuel cell will require less space than other fuel cells which allows for more available room for fuel to extend endurance of the aircraft. Coupling this with low operating temperature ranges between 50 and 100 °C and low noise level, which provides an ideal power source for a reconnaissance UAS, this will make the UAS powered by PEM fuel cell very difficult to be detected and hence targeted, as the most targeting systems rely on thermal tracking techniques for detecting and targeting aircrafts. However, PEM fuel cell suffers from slow response to the sudden changes in power demand which can be a problematic for aircrafts, as this will limit their dynamic performance [8].

Hwang et al. [9] developed a design of EAV-3 HALE UAS based on a solar-electric power supply. The EAV series of HALE UAS was designed to compete with the Qinetiq's Zephyr 7 the UAS with the longest flight time, with a target to stay in flight for up to 5 years [9]. The solar panel powered UAS is used for high altitude reconnaissance operation such as the PHASA-35 solar-powered UAS. Whilst, for low altitude flights, lithium-ion battery powered UAS is conventionally used such as the RQ-11 Raven [10]. However, it is difficult to obtain a robust design for a solar-powered UAS that is capable to endure a wider range of weather conditions in comparison with the PEM fuel cell-powered UAS [11]. Moreover, a PEM fuel cell-powered UAS has a potential for larger endurances than lithium-ion battery powered UAS. Meta Vista achieved a world record endurance of 12 h, utilising 6 L of liquid hydrogen cylinder and 800 W Intelligent Energy PEM fuel cell, with their commercial PEM fuel cell-powered UAS (The DJI M600) [12, 13]. Therefore, a PEM fuel cell-powered UAS could have a greater balance of the desired design requirements (e.g., endurance and robust) than a solar or lithium-ion-powered UAS. The world's best-selling commercial UAS is the DJI M600, which has a maximum take-off weight of 15 kg and a maximum payload weight of up to 2.5 kg and has an endurance of up to 2 h

whilst utilising Intelligent Energy's 2.4 kW PEM fuel cell [12, 14].

The Ion Tiger is the first practical UAS designed using fuel cell power developed by the US Naval Research Laboratory NRL. The design consists of a fuselage encapsulating the liquid hydrogen, wingspan of 5.18 m located at the top of the fuselage, and a cruciform empennage, with the aid of a horizontal stabiliser positioned half way up the vertical stabiliser all of which amounting to 16.78 kg, as shown in Fig. 1. The NRL recorded an unofficial flight time of 48 h for the Ion Tiger in 2013. The initial design has been developed to a new concept design, named as The Hybrid Tiger, which implemented the original Ion Tiger design utilising solar arrays located on the wings of the UAS. The Hybrid Tiger has a gross take-off mass (GTOM) of 25 kg, wingspan of 7.3 m, and about 2 days endurance. A high wing monoplane with a large lift/drag ratio of 21:1 can fly efficiently at 15 m/s. The frame of the aircraft accounts for less than 30% of total take-off mass and is made from a spread-tow carbon fibre and foam sandwich composite skin, which allows for a light-weight and robust design, and empty Hydrogen tank accounts for 33% of total take-off mass [11, 15].

For a large aircraft with wingspan 33.22 m, Tulapurkara et al. [16] used a fuselage length-to-wingspan ratio (l_f/b) of 1.05. Whereas, for a light-weight RC aircraft with a wingspan of 1.68 m, an l_f/b ratio of 0.75 was reported. There are two methods which are used to estimate the mass of an aircraft's fuselage; these are the Torenbeek and Affdl methods. Torenbeek's method is a default recommended choice and consists of breaking the mass of the fuselage down into categories (shell skin, stringers, bulkheads, supports, and floors); this method is sensitive to pressurisation levels and design load factors [17].

This paper will focus on examining the design requirements for an unmanned aircraft system based on 1-kW PEM fuel cell for high-altitude operation (10–11 km), which can be correlated into a quantitative data to produce a design constraints diagram, where there is a limited research in this area for small-scale UAS which is powered by the relatively new power source. In this research, the impact of changing the capacity of the power system on the design requirements of the UAS and the design constraints will be investigated, also the estimation of the power required for each flying segment and the potential endurance of 1 kW fuel cell system, and the impact of take-off distance up on the wing loading and stall speed of the proposed UAS design, and different wing geometries, will be examined and addressed.

Fig. 1 The Ion Tiger high endurance UAS developed by the US Naval Research Laboratory (cited from [15])

2 Power and mass estimation of unmanned aircraft system-based PEM fuel cell

For a PEM fuel cell-powered UAS, the power delivered by the propeller subjects to the efficiency of the PEM stack and the propeller [17]. To obtain maximum power output which the propeller delivers, efficiencies must be taken into account as given in Eq. 1 [18].

$$P_o = P_s \times \eta_m \times \eta_p \times \eta_{PEM} \tag{1}$$

where P_o represents maximum power delivered by the propeller, P_s is the power supplied to the motor in watts (W), η_m is the efficiency of motor, η_p is the efficiency of propeller, and η_{PEM} is the efficiency of PEM fuel cell stack. It has been assumed that the motor for UAS applications can have an efficiency of 85–95% [19, 20]. For a commercial aircraft, Sforza [21] claimed that propeller's efficiency is in the region of 82–92%, whereas Shariff [22] claimed in his research for a smaller aircraft with wingspan equal to 1.445 m; that an efficiency of 65–74% is achieved with the propeller. Gudmundsson [23] claimed that efficiency of the propeller varies throughout the different phases of the aircraft's flight. Saleh et al. [24, 25] claimed that for a 1 kW PEM fuel cell, Horizon operates at a maximum output of 877 W with a current rating of 20 A, achieving 87.7% efficiency. Therefore, in this research, the propeller efficiency is assumed to be 80%. The efficiency value can be applied to Eq. 1 above to generate the power delivered by the propeller.

$$P_{o(1kW)} = 1000 \times 0.877 \times 0.95 \times 0.80 = 666.52 \text{ W}$$

Saleh [26] reported that the whole flight of the aircraft can be split into three phases (climbing, cruising, and descending), estimated that a UAS-based 1 kW PEM power plant system needs 60 min to climb to the altitude of 36,000 ft. (11 km) at climbing speed of 11 km/h, with a 100% load power required for climbing phase which is found to be 877 W due to the operational efficiency of the stack. Whilst during the cruising phase, the drawn power from the fuel cell stack was assumed to be 65% of the maximum power plant capacity. Also, the UAS was assumed to

Table 1 Power requirements for each flight phase of the 1 kW PEM fuel cell systems [26]

Flying phases	1 kW PEM fuel cell stack		
	Fuel cell stack current (A)	Fuel cell output power (W)	Power delivered by propeller (W)
Climbing	20	877	666.126
Cruising	13	609	462.84
Descending	7	352	267.52

Table 2 Initial mass estimation of the main components for the 1 kW PEM fuel cell-powered UAS

Components	Mass (kg)
Aircraft body	10
Payload	1
PEM fuel cell (with fan and casing)	4
PEM fuel cell controller	0.4
Oxygen and hydrogen vessels	16.1
BLDC motor	0.396
Propeller	0.43
Electronics	0.5
Heater	0.3
Total	33.126

spend 45 min for descending from 11 km cruising altitude, with a drawn power to be 35% of the maximum power plant capacity. Accordingly, the power demand for 1 kW PEM fuel cell stack is determined as in Table 1.

To estimate the endurance of the flight, mass estimation of the UAS and the carried payload must be essentially determined. Saleh [26] reported that a total of 16.1 kg mass of hydrogen and oxygen vessels are required to operate a 1 kW PEM fuel cell system for 4 h cruising time at 11 km high-altitude UAS. The Hybrid Tiger's fuel container accounts for 33% of the maximum take-off mass of the aircraft; therefore, the mass estimate of the fuel container can be made when all other contributing masses are determined [11].

The estimated masses of the main components for the 1 kW PEM fuel cell-powered UAS as reported in the literature [19, 26–29] are presented in Table 2. To investigate the impact of changing the capacity of the power system on the design of the UAS, it is assumed the body of the aircraft weighs 10 kg for the 1 kW system. The total estimated mass of 33.12 kg for the 1 kW powered UAS will be adapted in this research to investigate the design requirements and the related constraints.

A maximum static thrust represents the maximum amount of thrust produced by the propeller, whilst the aircraft is still stationary. The maximum static thrust T_{sm} in (N) can be determined by Eqs. 2 and 3 [26].

$$T_{sm} = (2\rho \times A \times P_o^2)^{1/3} \tag{2}$$

$$A = \pi \left(\frac{P_d}{2} \right)^2 \tag{3}$$

where ρ is the density of air (kg/m^3), A is the area of the propeller rotation path (m^2), P_o is the power output of the propeller (W), and P_d is the propeller diameter (m). The maximum static thrust-to-weight ratio is given in Eq. 4 [30].

$$\text{Maximum Static Thrust to weight ratio} = \frac{T_{sm}}{M \times g} \tag{4}$$

where M is the mass in (kg) and g is the gravitational constant (9.8 m/s^2). If maximum static thrust-to-weight ratio can be assumed, hence the total permissible mass for the UAS can be determined. Greatrix [31] reported that most of the conventional fixed wing aircraft possess a maximum static thrust-to-weight ratio of 0.2–0.4. Using Eqs. 1–4 above to determine the maximum permissible mass of the UAS for the maximum static thrust-to-weight ratios of 0.2 and 0.4, respectively, based on 1 kW PEM Fuel Cell power systems, and for different propeller diameters, as presented in Fig. 2.

In general, a PEM fuel cell itself is a heavy component and the fuel tank itself even heavier therefore allowing for more total take-off mass [3]. Therefore, in this research, a maximum static thrust-to-weight ratio of 0.2 will be adapted, as it allows more mass for hydrogen fuelled PEM fuel cell-powered system to be carried, which will extend the endurance mission of the UAS.

3 Wing design calculations

The design calculation of the wing loading W/S (N/m^2) of the aircraft is mainly governed by the characteristics and boundaries of stall condition, take-off distance, total weight of the aircraft, and the power of the propulsion system, as given in Eqs. 5–7 [3].

$$V_{So} = \left(\frac{2 \times \frac{W}{S}}{\rho \times C_{Lmax}} \right)^{\frac{1}{2}} \tag{5}$$

$$\frac{HP}{W} = \frac{2.44}{550\eta_p} \times \frac{1}{gd_{to}} \left(\frac{1}{\rho C_{L_{max}}} \times \frac{W}{S} \right)^{\frac{3}{2}} \tag{6}$$

$$HP = \frac{P_o}{745.7} \tag{7}$$

where, ρ is the density of air at sea level (1.225 kg/m^3), C_{Lmax} is the maximum lift coefficient (assumed to be 1.0)

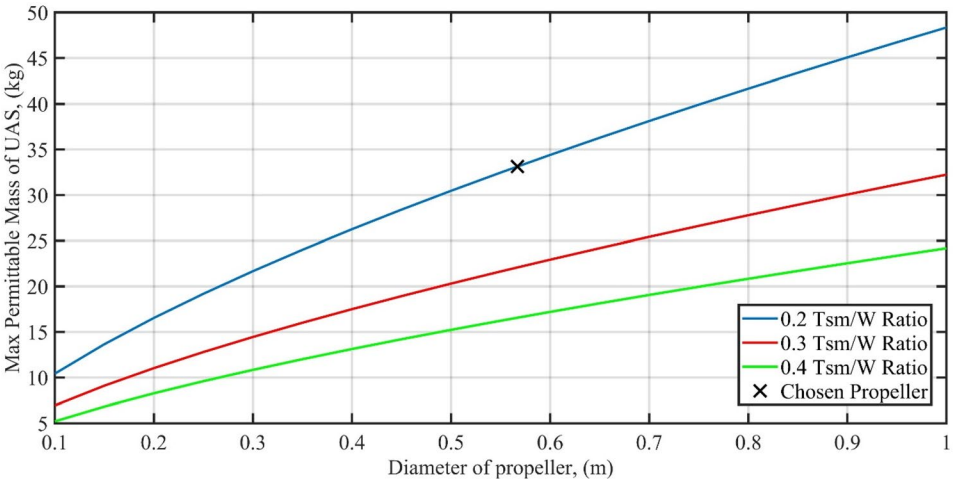

Fig. 2 Maximum permissible mass boundaries of UAS based on 1 kW PEM fuel cell, for different propeller diameters

[32, 33], V_{So} is the stall speed (m/s), HP is the generated horsepower (hp), W is the maximum take-off weight of the aircraft (N), η_p is the propeller efficiency, g is the gravitational constant (N), d_{to} is the take-off distance (m), and P_o is the power delivered by the propeller (W). The stall speed of the aircraft is the minimum speed at which a particular aircraft must fly at to satisfy (Lift > Take-off weight) and, therefore, stay aloft. Therefore, it is important to maintain flying speed of the aircraft beyond its design stall speed [34]. From Table 1, the power delivered by the propeller is 666.1 W (0.893 HP) for the 1 kW PEM fuel cell-powered UAS system, and using Eqs. 5–7, the relationship between take-off distance and wing loading can be determined and presented, as shown in Fig. 3, whilst the relationship between the wing loading and the stall speed is presented in Fig. 4.

It is clear that both of wing loading and stall speed can be significantly affected by the take-off distance; therefore, four different take-off distances (10, 40, 70, and 100 m) will be considered for further investigation in this research to determine their impact on wing geometries, resulting with four design geometries (A–D), as presented in Table 3.

To obtain a high lift-to-drag ratio, the wing area must be maximised whilst not compromising the aerodynamic shape of the wing. For a trapezoidal wing shape, as shown in Fig. 5, the most fundamental wing parameters can be determined by using Eqs. 8–12 [3].

$$\mathrm{AR} = \frac{b^2}{S} \tag{8}$$

$$\lambda = \frac{C_{\mathrm{tip}}}{C_{\mathrm{root}}} \tag{9}$$

$$W_s = \frac{W}{S} \tag{10}$$

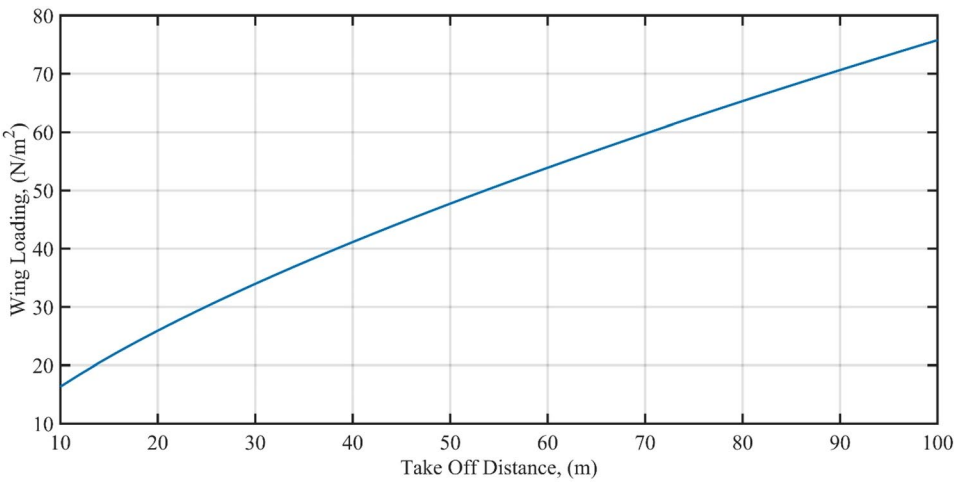

Fig. 3 Wing loading of UAS design for various take-off distances for a 1 kW PEM fuel cell system

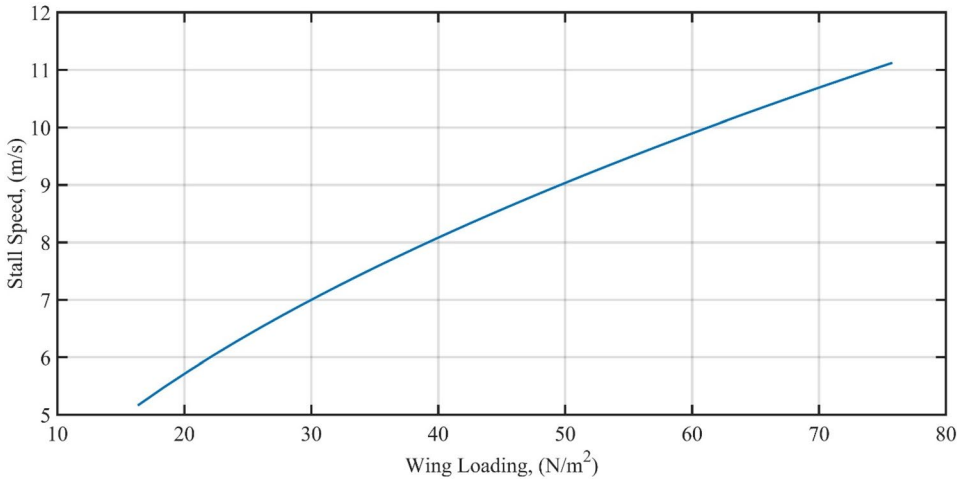

Fig. 4 Stall speed of UAS design for various wing loadings for a 1 kW PEM system

Table 3 Wing geometry of the initial UAS design of wing loading and stall speed for a 1 kW PEM system

Take-off distance (m)	Geometry	Wing loading (N/m^2)	Stall speed (m/s)
10	A	16.326	5.163
40	B	41.140	8.196
70	C	59.743	9.876
100	D	75.781	11.123

$$\mathrm{MAC} = \frac{2}{3}\left[\frac{C_{\mathrm{root}} + C_{\mathrm{tip}} - \left(C_{\mathrm{root}} \times C_{\mathrm{tip}}\right)}{C_{\mathrm{root}} + C_{\mathrm{tip}}}\right] \tag{11}$$

$$S = \frac{b\left(C_{\mathrm{root}} + C_{\mathrm{tip}}\right)}{2} \tag{12}$$

where AR represents the aspect ratio, b is the wingspan (m), S is the wing surface area (m^2), λ is the taper ratio, C_{tip} is the chord tip (m), C_{root} is the chord root (m), W_{s} is the wing loading (N/m^2), W is the maximum take-off weight (N), and MAC is the mean aerodynamic chord.

The cruise speed of the aircraft is the speed at which the aircraft travels when it reaches its level flying altitude, and in our case study, it is (10–11 km), whereas, the stall speed is the slowest speed the aircraft can travel whilst producing enough lift to maintain the required altitude. The aspect ratio governs the relation between the wingspan and the wing area which affects the manoeuvrability and robust nature of the aircraft. A relatively low aspect ratio allows the aircraft to have greater manoeuvrability and will give the UAS a greater practicality for fuel storage and space for the fuel cell in the fuselage; however, for HALE missions, UAS typically have a high aspect ratio of approximately 25 [35]. Kody et al. [36] investigated a small UAV design of less than 10 m wingspan, which reported that both high and low aspect ratios are both positive; therefore, a further investigation can be carried out to determine the most efficient value. The taper ratio shows the change in width of the wing which was also designed to fall between 0.4 and 0.5 leads to the greatest efficiency for a trapezoidal wing; however, the taper ratio directly affects the Oswald Efficiency; therefore, this is a very important component to be considered [3]. The Oswald efficiency acts as a correction factor which represents the changes in drag and lift of a three-dimensional wing aircraft, in comparison with an ideal wing having the same aspect ratio and an elliptical lift distribution [3]. Many parameters have been assumed and given in the literature to obtain the dimensional geometries of the wing [3, 23, 32, 33, 35, 37], as presented in Table 4.

For the aluminium alloy wing design, the weight of the wings can be determined using a thickness-to-chord ratio as given in Eqs. 13 and 14, respectively [7, 38].

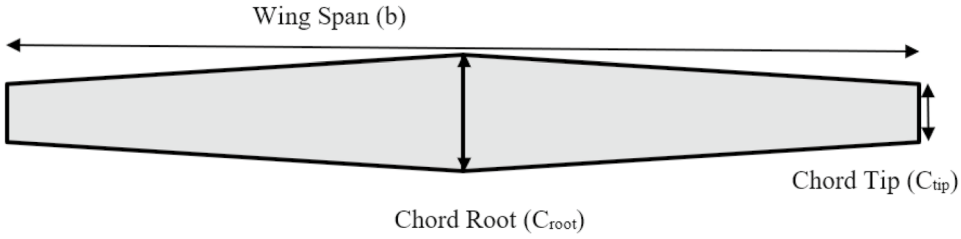

Fig. 5 A trapezoidal of wing shape

Table 4 Assumptions for obtaining initial wing geometry parameters

Wing parameters	Size	Unit
Maximum lift coefficient	1.0	N/A
Aspect ratio	25	N/A
Taper ratio	0.5	N/A
Mach no	0.05	N/A
Oswald efficiency	0.8	N/A
Propeller efficiency	0.8	N/A

$$\text{Thickness to Chord Ratio} = \frac{T_{\text{root}}}{C_{\text{root}}} \tag{13}$$

$$W_{\text{wing}} = 110 \times \left[\frac{M_{\text{TOM}} N_{\text{ult}} bS}{T_{\text{root}}}\right]^{0.77} \times 10^{-6} \tag{14}$$

where C_{root} is the chord root (ft), T_{root} is the theoretical root thickness (ft), W_{wing} is the mass of wing (lbs), M_{TOM} is the maximum take-off mass (lbs), N_{ult} is the ultimate load factor, b is the wingspan (ft), and S is the wing surface area (ft^2). N_{ult} is the design limit load multiplied by a safety factor whereby the design limit load is the maximum load that the aircraft can sustain before failure occurs [39]. In this research, N_{ult} will be assumed to be 2.5 [40]. Ramos [41] reported that a thickness-to-chord ratio of 0.14 is the most efficient value for light-weight aircraft.

4 Fuselage design estimation

The fuselage length (l_{f}) can be estimated using the wingspan of the aircraft (b) as given in Eq. 15 [16]. For a large aircraft with a wingspan 33.22 m, Tulapurkara et al. [16] used a fuselage length-to-wingspan ratio (l_f/b) of 1.05. Whereas, for a light-weight glider with a wingspan of 50–60 cm, a (l_f/b) ratio of 0.65–0.75 is utilised. In this research, given the size and weight of the aircraft geometries, a (l_f/b) ratio of 0.75 will be adopted.

$$\text{Fuselage length to wingspan ratio} = \frac{l_f}{b} \tag{15}$$

where l_{f} is the length of fuselage (m) and b is the wingspan (m). The corresponding width for various fuselage lengths can be found by applying a fineness ratio FR; the fineness ratio governs the relation between the length and the average diameter of the aircraft, as given in Eq. 16 [3]. Theoretically, the ideal fineness ratio for a subsonic aircraft is given to be equal to 6; however, this can vary due to internal size requirements; a practical value for most common aircraft is 8 [42]. However, the main area where the diameter could create problems in the UAS design is its capability to contain the hydrogen fuel tank and the PEM fuel cell system. Therefore, in this research, a fineness ratio of 8 will be used for this initial design purpose.

$$\text{FR} = \frac{l_f}{D_{\text{ave}}} \tag{16}$$

where l_{f} is the length of fuselage (m) and D_{ave} is the average diameter of fuselage (m). Using Eqs. 8–16, the design parameters and geometries of the UAS power by a 1 kw PEM fuel cell system can be determined as presented in Table 5.

It can be noticed that Geometry D offers the greatest stall speed and the smallest possible wing mass, fuselage's length, and diameter, thus will be further investigated for weight approximations as this design offers a higher permissible mass for extra fuel and hence longer endurances.

There are two methods which are used to estimate the mass of an aircraft's fuselage; these are the Torenbeek and Affdl methods [16]. Torenbeek's method breaks the fuselage mass down to interior and exterior components of the fuselage; Torenbeek's method offers a greater accuracy of estimation and takes into account the interior walls of the aircraft; therefore, this method will be adopted to find out the shell mass of the fuselage; this can be determined by Eqs. 17–21 [17].

$$W_{\text{G}} = W_{\text{sk}} + W_{\text{str}} + W_{\text{fr}} \tag{17}$$

$$W_{\text{sk}} = 0.05428 \times K_{\lambda} \times {S_{\text{G}}}^{1.07} \times {V_{\text{D}}}^{0.743} \tag{18}$$

$$K_{\lambda} = 0.56 \times \left(\frac{l_t}{b_f + h_f}\right)^{3/4} \tag{19}$$

$$W_{\text{str}} = 0.0117 \times K_{\lambda} \times {S_{\text{G}}}^{1.45} \times {V_{\text{D}}}^{0.39} \times {n_{\text{ult}}}^{0.316} \tag{20}$$

For $(W_{sk} + \text{Wstr}) < 286$ kg,

$$W_{\text{fr}} = 0.0911 \times \left(W_{\text{sk}} + W_{\text{str}}\right)^{1.13} \tag{21}$$

where W_{G} is the gross shell mass (kg) of the fuselage, W_{sk} is the gross skin mass (kg), W_{str} is the gross stringer and longeron mass (kg), W_{fr} is the gross frame mass (kg), K_{λ} is the correction factor of the shell mass, S_{G} is the gross shell area (m^2), V_{D} is the design dive speed (m/s), l_{t} is the distance between the ¼ chord points of the wing root and the horizontal (m), b_{f} is the maximum width of fuselage (m), h_{f} is the maximum depth of fuselage (m), and N_{ult} is the ultimate load factor [17].

By applying Torenbeek's fuselage mass estimation method represented in Eqs. 17–21 on the design of geometries D above, and assuming the shell area of the fuselage S_G is a regular continuous cylinder without variation in shape as

Table 5 UAS design parameters powered by a 1 kW PEM fuel cell system

Geometry	Take-off distance (m)	Wing loading (N/m^2)	Stall speed (m/s)	Wing surface Area (m^2)	Wingspan (m)	C_{root} (m)	C_{tip} (m)	Wing mass (kg)	Fuselage length (m)	Fuselage diameter (m)
A	10	16.326	5.163	19.905	22.307	1.494	0.747	26.60	16.73	2.09
B	40	41.140	8.196	7.889	14.053	0.749	0.375	15.53	10.54	1.32
C	70	59.743	9.876	5.439	11.661	0.622	0.311	11.67	8.75	1.09
D	100	75.781	11.123	4.288	10.354	0.552	0.276	9.72	7.77	0.97

Table 6 Estimated masses of the main components for the 1 kW PEM fuel cell-powered UAS

Components	Mass (kg)
Aircraft body	11.66
Payload	1
PEM fuel cell (with fan and casing)	4
PEM fuel cell controller	0.4
Oxygen and hydrogen vessels	16.1
BLDC motor	0.396
Propeller	0.43
Electronics	0.5
Heater	0.3
Total	34.786

this is an initial estimate. Dive speed (V_D) is the maximum speed that the aircraft should fly. It has been reported that the design dive speed is generally 1.25 times larger than cruising speed [43]. The cruising speed for the 1 kW designed aircraft is assumed to be equal to 20 m/s; therefore, for geometry D, V_D is equal to 25 m/s; using Eqs. 17–21 to determine the gross mass of the fuselage W_G which is found to be equal to 1.94 kg. Adding the mass of the wing from Table 5 to the gross fuselage mass to obtain the total body mass of the UAS which becomes (9.72 + 1.94 = 11.66 kg) for the geometry D design. By substituting the new mass estimations into the initial estimated masses of Table 2, resulting Table 6.

Given the maximum permissible mass of the aircraft powered by a 1 kW fuel cell system is equal to 33.126 kg as shown in Table 2, however, in Table 6, there is a about 1.66 kg of extra mass; this will come on the cost of reducing the amount of hydrogen and oxygen to avoid exceeding maximum take-off mass of 33.126 kg.

5 Design constraints

The design constraints of the system are very vital to determine the maximum and minimum limitation border of the system operation and performance, thus will enable the designer to choose the optimum design that fulfils the mission requirements. Gudmunsson [23] presented set of equations that can be used to construct a design constraint diagram, these express the minimum thrust required to achieve the desired requirements of the aircraft such as: *T/W* for a level constant velocity turn, *T/W* for a desired rate of climb, *T/W* for a desired cruise UAS speed, and finally *T/W* for a desired service ceiling for a propeller aircraft, which determines the maximum altitude that can reached. Eqs. 22–27 express these constraints [23].

Level constant maneuvering

$$\frac{T}{W} = q\left[\frac{C_{\mathrm{Dmin}}}{(W/S)} + k\left(\frac{n}{q}\right)^2\left(\frac{W}{S}\right)\right] \tag{22}$$

Desired rate of climb

$$\frac{T}{W} = \frac{V_{\mathrm{V}}}{V} + \frac{q}{(W/S)}C_{\mathrm{Dmin}} + \frac{k}{q}.\left(\frac{W}{S}\right) \tag{23}$$

Desired cruise

$$\frac{T}{W} = qC_{\mathrm{Dmin}}\left(\frac{1}{W/S}\right) + k\left(\frac{1}{q}\right)\left(\frac{W}{S}\right) \tag{24}$$

Desired service ceiling

$$\frac{T}{W} = \frac{V_V}{\sqrt{\frac{2}{\rho}\left(\frac{W}{S}\right)\sqrt{\frac{k}{3.C_{\mathrm{Dmin}}}}}} + 4\sqrt{\frac{k.C_{\mathrm{Dmin}}}{3}} \tag{25}$$

$$q = \frac{1}{2}\rho V^2 \tag{26}$$

$$k = \frac{1}{\pi \times AR \times e} \tag{27}$$

where T/W is the thrust-to-weight ratio, q is the dynamic pressure (kg/m^2), C_{Dmin} is the minimum drag coefficient, k is the lift induced drag constant, N is the ultimate load factor, W/S is the wing loading (kg/m^2), V_{V} is the vertical speed (m/s), V is the cruising speed (m/s), ρ is the density of air at ceiling altitude (kg/m^3), and e is the Oswald efficiency number. The assumptions for constraint calculations for the UAS power by a 1 kW PEM fuel cell system are as given in Table 7, by substituting the values of Table 7 in Eqs. (22–27) to determine the relation between thrust-to-weight ratio T/W and the wing loading W/S of the design as presented in Fig. 6.

Figure 6 allows the designer to narrow down the range of possible designs for the UAS given initial assumptions and requirements. The plots represent the minimum thrust-to-weight ratio required to achieve each of the respected requirements of the UAS (listed in the legend of Fig. 6). The constraints diagram shows the service ceiling (green line) which requires the most thrust. However, the intersect of the 0.2 T/W and 75.78 wing loading W/S is determined in Table 5 (Geometry D) which represents the current design estimations of the UAS (shown as a cross X) in Fig. 6; this is below the minimum thrust-to-weight ratio to achieve the desired service ceiling. This could be rectified through further alterations and adjustments to the design and mission requirements, so that the design of the UAS will fall within the possible design space. To achieve this, the following actions could be taken as listed below in order of effectiveness:

1. Reduce the maximum take-off mass of the UAS, the fuel and fuel container are the heaviest components of the UAS design and are flexible parameters. Further investigations to examine any optimisation of shape could be carried out to reduce its maximum take-off mass.
2. Slightly lowering the cruising altitude, this would lower the required thrust-to-weight ratio which would mean

Table 7 Assumptions for UAS constraint calculations for a 1 kW PEM system

Parameters	Values
C_{Dmin} [21]	0.032
N [21]	2.5
V_{V}	3 m/s
V	20 m/s
ρ [17]	0.365 kg/m^3
e [22]	0.80
AR	25

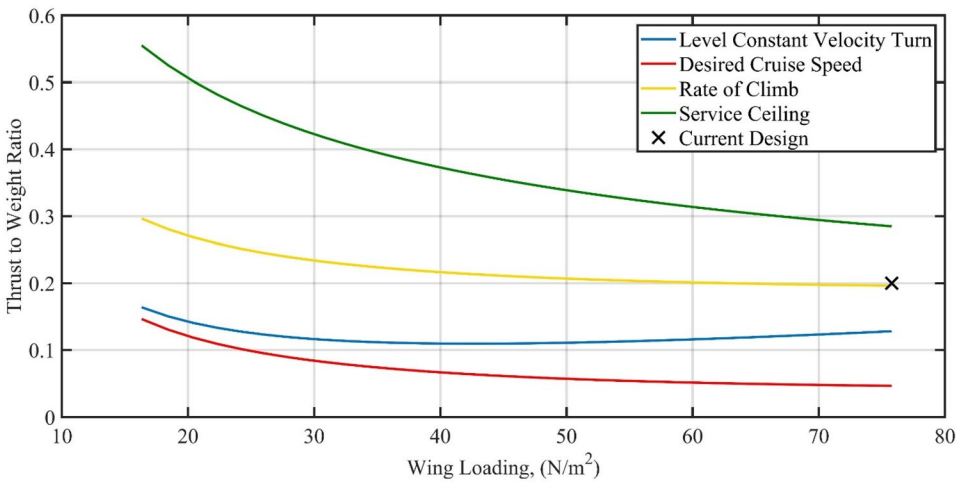

Fig. 6 Design constraints for the 1 kW PEM fuel cell-powered UAS

less thrust is required to reach the possible design area for the UAS design.
3. The aspect ratio could be decreased as well; however, the aspect ratio would similarly reduce the required thrust-to-weight ratio required to achieve the desired service ceiling.

6 Conclusion

In this paper, the design requirements of a UAS system powered by a 1 kW PEM fuel cell system for high-altitude operation (10–11 km) are presented, which has been correlated into the design constraints diagram. The impact of changing the capacity of the power system, take-off distance up on the wing loading, and stall speed of the proposed UAS design and wing geometries, on the design and mission requirements of the UAS and the design constraints, are investigated. A static thrust-to-weight ratio of 0.2 was selected as this allowed for a greater permissible mass for the aircraft, which yielded static thrusts of 65 N for the 1 kW PEM fuel cell system. The wing and fuselage dimensions and masses, as well as several other design features, are investigated. The design parameters of the proposed UAS yielded an aircraft of maximum take-off mass 34.8 kg, wingspan of 10.4 m, cruising speed 20 m/s, stall speed 11.23 m/s, and maximum endurance of 4 h. However, the initial mass estimation of the UAS design was found equal to 33.126 kg, whilst the final mass estimation design is found to be 34.8 kg, which is within acceptable tolerance. From the design constraint diagram, it has been concluded that the proposed design estimations of the UAS fall below the minimum thrust-to-weight ratio to achieve the desired service ceiling; however, further alterations and adjustments on the design and mission requirements are provided to place the design of the UAS within the possible design space. The wing and fuselage mass estimations use methods which are generically used for large aircraft and made of aluminium alloy; therefore, validation of these estimations' accuracy for smaller scale aircraft of (< 100 kg) would improve the accuracy of the calculations that are affected by the wing and fuselage mass estimations in this research.

Acknowledgements The authors would like to thank School of Engineering at the University of Lincoln for their technical support.

Author contributions The first author contributed to this paper through conducting the relevant literature survey, developing the design of the aircraft, examining and analysing the relevant involved parameters, and visualising the results. Whilst the second author was responsible in supervising and directing the research activities and also drafting and revising the content of this paper.

Funding The authors declare that there is no financial or non-financial conflict of interest.

Data availability The authors declare that all the data and the relevant materials are presented in the manuscript; there are no further data that can be solely requested in the future.

Code availability The authors declare the MATLAB script that has been developed to produce the results of this research will not be available for future request.

Declarations

Conflict of interest The authors declare that they have no conflict of interests.

Ethics approval The authors declare that no ethical approval is required for this research.

Consent to participate This research has non-human subjects' involvement; hence, a consent to participate is not required.

Consent for publication The authors declare that no consent is required to be obtained from individuals as there are no human subjects involved.

References

1. SKYbrary. *Unmanned Aerial Systems (UAS)*. 2019 cited 02/12/2019. www.skybrary.aero/index.php/Unmanned_Aerial_Systems_(UAS).
2. Defense OotSo (2002) UAV Roadmap 2002.
3. Kundu AK (2010) Aircraft design. 27. Cambridge University Press.
4. Howe D, Rorie G (2000) Aircraft conceptual design synthesis. Professional Engineering Publishing London, UK.
5. Tsach S, Yaniv A, Avni H, Penn D (1996) High altitude long endurance (HALE) UAV for intelligence missions. In: ICAS Proceedings.
6. Altman A (1998) Design methodology for low speed high altitude long endurance unmanned aerial vehicles.
7. Dababneh O, Kipouros T (2018) A review of aircraft wing mass estimation methods. Aerosp Sci Technol 72:256–266.
8. Verstraete D, Lehmkuehler K, Gong A, Harvey JR, Brian G, Palmer JL (2014) Characterisation of a hybrid, fuel-cell-based propulsion system for small unmanned aircraft. J Power Sources 250:204–211.

9. Hwang S-J, Kim S-G, Kim C-W, Lee Y-G (2016) Aerodynamic design of the solar-powered high altitude long endurance (HALE) unmanned aerial vehicle (UAV). Int J Aeronaut Space Sci 17(1):132–138.
10. Air Force Technology. PHASA-35 Solar-Powered HALE UAV. 2018 cited 23/02/2020. http://www.airforce-technology.com/projects/phasa-35-solar-powered-hale-uav/.
11. Stroman R, Edwards D, Jenkins P, Carter S, Newton D, Kelly M, Heinzen S, Young T, Dobrokhodov V, Langelaan J. The hybrid tiger: A long endurance solar/fuel cell/soaring unmanned aerial vehicle. In:48th power sources conference. 2018.
12. Meta Vista. *"What we do"* 2019 cited 01/12/2019. https://metavistausa.com.
13. Intelligent Energy. *News & Events: Intelligent Energy*. 2019 cited 02/12/2019. Available from: https://www.intelligent-energy.com/news-and-events/company-news/2019/04/16/metavista-breaks-guinness-world-record-of-multi-rotor-uav-flight-time-using-intelligent-energy-fuel-cell-power-module/#:~:text=Loughborough%2C%20Tuesday%2016%20April%202019,World%20Record%20of%20flight%20time.
14. DJI. Matrice 600. 2019 cited 02/12/2019. www.dji.com/uk/matrice600/info.
15. Technology N Ion Tiger UAV. 2009 cited 03/12/2019. https://www.naval-technology.com/projects/ion-tiger-uav/#:~:text=Ion%20Tiger%20is%20a%20liquid,and%20pollution%2C%20making%20them%20detectable.
16. Tulapurkara E, Venkattraman A, Ganesh V (2007) An example of airplane preliminary design procedure–jet transport. Report No AE TR 4:106.
17. Torenbeek E Synthesis of subsonic airplane design: an introduction to the preliminary design of subsonic general aviation and transport aircraft, with emphasis on layout, aerodynamic design, propulsion and performance. 2013: Springer Science & Business Media.
18. Chung P-H, Ma D-M, Shiau J-K (2019) Design, manufacturing, and flight testing of an experimental flying wing UAV. Appl Sci 9(15):3043.
19. Models, R. KMS Quantum 4130/09 Brushless Motor. cited 20/01/2020. http://radioactivemodels.ie/shop/product_info.php?products_id=432.
20. MIT. Performance of Propellers. cited 20/01/2020. https://web.mit.edu/16.unified/www/FALL/thermodynamics/notes/node86.html.
21. Sforza PM (2014) Commercial airplane design principles. Elsevier.
22. Shariff MF (2007) Propeller aerodynamic analysis and design. RMIT University.
23. Gudmundsson S (2013) General aviation aircraft design: Applied Methods and Procedures. Butterworth-Heinemann.
24. Saleh M, Ali IMR, Zhang H (2016) Simplified mathematical model of proton exchange membrane fuel cell based on horizon fuel cell stack. J Modern Power Syst Clean Energy, 4(4): 668–679.
25. Saleh M, Ali IMR, Zhang H (2018) Experimental testing and validation of the mathematical model for a self-humidifying PEM fuel cell. J Mater Sci Chem Eng 6(4): 202–218.
26. Salah M, IM, Modelling, simulation and performance evaluation: PEM fuel cells for high altitude UAS. 2016, Sheffield Hallam University.
27. Store FC Horizon PEM Fuel Cell H-1000/Manuals/Fuel Cell Store. 2015 cited 26/01/2020. http://www.fuelcellstore.com/manuals/horizon-pem-fuel-cell-h-1000-manual.pdf.
28. Supplies NM Graupner E-Prop Electric Propeller 15x8" 1326.15X8. cited 10/01/2020. http://www.nexusmodels.co.uk/graupner-e-prop-electric-propeller-15x8-1326-15x8.html.
29. Pentair. Touch-Safe Heaters cited 09/03/2020. www.farnell.com/datasheets/2133638.pdf.
30. Nancy Hall. Thrust to Weight Ratio. 2015 cited 01/04/2020. www.grc.nasa.gov/www/k-12/airplane/fwrat.html.
31. Greatrix DR Powered Flight. 2012: Springer.
32. Russell J (1996) Performance and stability of aircraft. Butterworth-Heinemann.
33. Körpe DS, Kanat ÖÖ (2019) Aerodynamic optimization of a UAV wing subject to weight, geometric, root bending moment, and performance constraints. Int J Aerospace Eng 2019.
34. Szirtes T (2007) Applied dimensional analysis and modeling. Butterworth-Heinemann.
35. Nickol CL, Guynn, MD, Kohout LL, Ozoroski TA (2007) High altitude long endurance UAV analysis of alternatives and technology requirements development.
36. Kody F, Bramesfeld G (2012) Small UAV design using an integrated design tool. Int J Micro Air Vehicles 4(2):151–163.
37. Nikiforow K, Pennanen J, Ihonen J, Uski S, Koski P (2018) Power ramp rate capabilities of a 5 kW proton exchange membrane fuel cell system with discrete ejector control. J Power Sources 381:30–37.
38. Murphy N (1987) Analytical wing weight prediction/estimation using computer based design techniques.
39. Wijker JJ (2008) Spacecraft structures. Springer Science & Business Media.
40. Administration (2016) U.S.D.o.T.-F.A., Pilot's Handbook of Aeronautical Knowledge.
41. Ramos M (2015) Construction and Analysis of a Lightweight UAV Wing Prototype. MS thesis, Técnico Lisboa, Lisbon, Portugal.
42. Roskam J (2002) Airplane design: Part III: Layout design of cockpit, fuselage, wing and empennage: Cutaways and inboard profiles. University of Kansas.
43. Duncan JS (2016) Pilot's Handbook of Aeronautical Knowledge. 2016, U.S. Department of Transportation, Fedral Aviation Admistration.